Carbohydrate Polymers 87 (2012) 667–675

Contents lists available at SciVerse ScienceDirect

Carbohydrate Polymers

journal homepage: www.elsevier.com/locate/carbpol

Separation, structure characterization, conformation and immunomodulating effect of a hyperbranched heteroglycan from Radix Astragali

Jun-Yi Yin[a,b,1], Ben Chung-Lap Chan[a,1], Hua Yu[a], Iris Yuen-Kam Lau[a], Xiao-Qiang Han[a], Sau-Wan Cheng[a], Chun-Kwok Wong[a,d], Clara Bik-San Lau[a], Ming-Yong Xie[b,**], Kwok-Pui Fung[a], Ping-Chung Leung[a], Quan-Bin Han[a,c,*]

[a] State Key Laboratory of Phytochemistry and Plant Resources in West China (CUHK), Institute of Chinese Medicine, The Chinese University of Hong Kong, Shatin, NT, Hong Kong, China
[b] State Key Laboratory of Food Science and Technology, Nanchang University, Nanchang 330047, China
[c] School of Chinese Medicine, Hong Kong Baptist University, Hong Kong, China
[d] Department of Chemical Pathology, The Chinese University of Hong Kong, Prince of Wales Hospital, Shatin, NT, Hong Kong, China

ARTICLE INFO

Article history:
Received 30 June 2011
Received in revised form 3 August 2011
Accepted 17 August 2011
Available online 24 August 2011

Keywords:
Radix Astragali
Polysaccharide
Structure character
Morphology feature
Immunomodulating effect

ABSTRACT

A water soluble polysaccharide (RAP) was isolated and purified from Radix Astragali and its structure was elucidated by monosaccharide composition, partial acid hydrolysis and methylation analysis, and further supported by FT-IR, GC–MS and ^{1}H and ^{13}C NMR spectra, SEM and AFM microscopy. Its average molecular weight was 1334 kDa. It was composed of Rha, Ara, Glc, Gal and GalA in a molar ratio of 0.03:1.00:0.27:0.36:0.30. The backbone consisted of 1,2,4-linked Rha*p*, α-1,4-linked Glc*p*, α-1,4-linked GalA*p*6Me, β-1,3,6-linked Gal*p*, with branched at *O*-4 of the 1,2,4-linked Rha*p* and *O*-3 or *O*-4 of β-1,3,6-linked Gal*p*. The side chains mainly consisted of α-T-Ara*f* and α-1,5-linked Ara*f* with *O*-3 as branching points, having trace Glc and Gal. The terminal residues were T-linked Ara*f*, T-linked Glc*p* and T-linked Gal*p*. Morphology analysis showed that RAP took random coil feature. RAP exhibited significant immunomodulating effects by stimulating the proliferation of human peripheral blood mononuclear cells and enhancing its interleukin production.

1. Introduction

Radix Astragali (*Astragalus*) is the dried root of *Astragalus membranaceus* (Fisch.) Bunge and *Astragalus mongholicus* Bunge (Fabaceae). It has been used in the treatment of various renal diseases in Traditional Chinese Medicine for over 2000 years. Modern researches showed that Radix Astragali possesses a variety of activities, including immunomodulating (Bedir, Pugh, Calis, Pasco, & Khan, 2000), anti-hyperglycemic (Chan, Lam, Leung, Che, & Fung, 2009), anti-inflammation (Choi et al., 2007), anti-oxidation (Yu, Bao, Wei, & An, 2005), antiviral activities (Zhu et al., 2009), etc.

Besides saponins and isoflavonoids, polysaccharides are believed as the principle active constituents of Radix Astragali (Chu, Qi, Li, Gao, & Li, 2010), which could activate the proliferation and cytokine production of mouse B cells and macrophages (Shao et al., 2004), and showed immunomodulating effects on Peyer's patch immunocompetent cells (Kiyohara et al., 2010). The crude polysaccharide could stimulate macrophages to express iNOS gene through the activation of NF-κB/Rel (Lee & Jeon, 2005). It could also ameliorate the digestive and absorptive function and regulate amino acid metabolism to beneficially increase the entry of dietary amino acid into the systemic circulation (Yin et al., 2009). An acid polysaccharide from Radix Astragali showed significant reticuloendothelial system-potentiating activity (Shimizu, Tomoda, Kanari, & Gonda, 1991).

Scientists made efforts in the structure characterization of the polysaccharides isolated from Radix Astragali (Kiyohara et al., 2010; Shao et al., 2004; Wang, Shan, Wang, & Hu, 2006) and only several glucans (Fang & Wagner, 1988; Li & Zhang, 2009) were well characterized. As for heteroglycans, nothing but monosaccharide composition and molecular weight was reported (Yan et al., 2010; Zhang et al., 2011). Therefore, their structures deserve further study.

Herein we report the isolation and purification of a water-soluble hyperbranched heteroglycan (coded RAP) from Radix Astragali. Its structure was characterized by a combination of chemical and instrumental analysis of monosaccharide compositions, methylation, partial acid hydrolysis, FT-IR, ESI-MS, GC–MS and

* Corresponding author. Tel.: +852 34112906.
** Corresponding author. Tel.: +86 791 83969009.
E-mail addresses: myxie@ncu.edu.cn (M.-Y. Xie), simonhan@hkbu.edu.hk (Q.-B. Han).
[1] Equal contribution.

0144-8617/$ – see front matter © 2011 Elsevier Ltd. All rights reserved.
doi:10.1016/j.carbpol.2011.08.045

NMR. Its morphology feature was further analyzed by scanning electron microscopy (SEM) and atomic force microscopy (AFM). RAP exhibited immunomodulating effects on human peripheral blood mononuclear cells.

2. Materials and methods

2.1. Material

The roots of *A. membranaceus* were purchased from herbal store in Hong Kong and identified by Dr. Chun-Feng Qiao. The voucher specimens are deposited at the Institute of Chinese Medicine, the Chinese University of Hong Kong, with voucher specimen number 2010-3268.

Hiload 26/60 Superdex-200 prep grad was purchased from Pharmacia Co. (Uppsala, Sweden). The dextran standards (T-2000, T-270, T-80, T-50, T-25 and T-12 with molecular masses of 2,000,000, 270,000, 80,000, 50,000 and 12,000 respectively) and monosaccharide standards of D-mannose (Man), L-rhamnose (Rha), D-galactose (Gal), D-arabinose (Ara), and D-glucose (Glc) were obtained from Merck Co. (Darmstadt, Germany). Ultra-pure water was produced by a Milli-Q water purification system (Millipore, Bedford, MA, USA). Lipopolysaccharide (LPS) was purchased from Sigma (St. Louis, USA). All chemical reagents were of analytical grade.

2.2. Extraction and purification of polysaccharide

The air-dried Radix Astragali (100 g) was cut into pieces and extracted twice with boiling water (2× 1.2 L) for 1 h. The solution was filtered and concentrated under reduced pressure. The solution was precipitated with four volumes of absolute ethanol for 12 h. The precipitate was resolved again in water and deproteined using Sevag method (Staub, 1965) for five times. Then the solution was dialyzed against distilled water for 72 h. Finally, the retentate was lyophilized with Virtis Freeze Dryer (The VirTis Company, New York, USA) to yield crude polysaccharide (RACP, 1.67 g).

RACP was dissolved in distilled water (4 mg/mL), filtered through a 0.45 μm membrane and separated by the Buchi Purifier system (BUCHI Labortechnik AG, Switzerland) coupled with a Hiload 26/60 Superdex-200 (2.6 cm × 60 cm) column, eluted with water at a flow rate of 2 mL/min. Fractions were collected every 3 min and checked using phenol-sulfuric acid under UV detection at 490 nm. Gel permeation chromatography (GPC) was used to test the homogeneity of the purified polysaccharide.

Total carbohydrate was determined using the phenol-sulfuric acid colorimetric method (Dubois, Gilles, Hamilton, Rebers, & Smith, 1956). Uronic acid contents were determined according to Blumenkrantz and Asboe-Hansen's method (Blumenkr & Asboehan, 1973). Protein was estimated by photometric assay using bovine serum albumin as the standard (Bradford, 1976). Specific rotation was recorded with a Perkin-Elmer 241 M digital polarimeter.

2.3. Homogeneity and molecular weight

The homogeneity and molecular weight of the purified polysaccharide was determined by GPC. It was analyzed on a Waters UPLC system (Waters, Milford, MA) equipped with a Waters Ultrahydrogel™ 1000 column (7.8 mm × 300 mm), a Waters ELS Detector, controlled with a Binary Solvent Manager system. The ELS Detector conditions were as follows: drift tube temperature (75 °C), nebulizer temperature (48 °C), gain (300 °C), gas pressure (45 Psi). Dextran standards with different molecular weight were used to calibrate the column and establish a standard curve.

2.4. Monosaccharide composition analysis

RAP was hydrolyzed with 2 M trifluoroacetic acid (TFA) at 120 °C for 2 h in a sealed test tube. The acid was removed under reduced pressure by repeated evaporation with methanol, and then the hydrolysate was converted into alditol acetates (Chen, Xie, Nie, Li, & Wang, 2008; Jones & Albersheim, 1972). Shimadzu GC/MS-QP2010 equipment (Nishinokyo Kuwabaracho, Kyoto, Japan) was used for the identification and quantification of monosaccharides.

2.5. Methylation and GC–MS analysis

2.5.1. Reduction of polysaccharide

The reduction of the uronic acid was conducted following a procedure as described in the literature (Taylor & Conrad, 1972) with slight modifications. RAP (20 mg) was added into water and treated with 1-cyclohexyl-3-(2-morpholinoethyl)-carbodimide methyl-p-toluenesulfonate (CMC) for five times, until the reduction of uronic acid completed. The polysaccharide after reduction (RAP-R) was subjected to monosaccharide composition and methylation analysis.

2.5.2. Methylation and GC–MS analysis

Methylation analysis of polysaccharide (RAP and RAP-R) was conducted according to the reported methods (Ciucanu & Kerek, 1984; Guo, Cui, Wang, & Christopher Young, 2008) with some modifications. The dried polysaccharide was dissolved in anhydrous dimethyl sulphoxide. Dry sodium hydroxide (30 mg) was added, and the mixture was stirred for 3 h at room temperature. Methyl iodide was added into the mixture. The reaction was stopped by adding water. The methylated polysaccharides were then extracted with chloroform followed by washing with distilled water for three times. They were acetylated with acetic anhydride to obtain partially methylated alditol acetates (PMAA).

GC/MS analysis of PMAA was performed on a DB-5 ms capillary column (0.25 μm × 0.25 μm × 30 m) using a temperature programming of 140 °C (3 min) to 250 °C (40 min) at 2 °C/min. Helium was used as the carrier gas. The components were identified by a combination of the main fragments in their mass spectra and relative GC retention times, comparing with the literature (Wang, He, & Huang, 2007).

2.6. Partial acid hydrolysis

RAP (50.5 mg) was treated with 0.05 M TFA (10 mL) at 100 °C for 1 h. The product was concentrated by evaporation of TFA with methanol, and then dialyzed against distilled water (5× 500 mL, molecular weight 3500 Da cut off). The solution outside of the dialysis bag (RAP-P-L) was collected for monosaccharide analysis and ESI-MS. The solution in the dialysis bag (RAP-P-H) was concentrated and lyophilized. RAP-P-H's homogeneity was confirmed by GPC. It was further applied to monosaccharide compositions and methylation analysis.

2.7. FT-IR analysis

Infrared spectra were recorded with a Thermo Nicolet 5700 infrared spectrometer (Madison, WI, USA), using KBr disks method.

2.8. NMR spectroscopy

RAP was treated with deuterium by lyophilizing with D_2O for three times. The deuterium-exchanged RAP (25 mg) was put in a 5-mm NMR tube and dissolved in 0.5 mL of 99.9% D_2O. NMR-spectra were recorded with a Brucker AM-600 NMR (Karlsrhue, Germany).

2.9. Molecular morphology analysis

Polysaccharide powder was placed on the sample stage, and coated with a thin layer of gold in a MODEL IB-3 ion coater (Eiko Corp., Mito City, Japan). Then it was examined in a QUANTA 200F scanning electron microscope (FEI Company, Holland). The sample was viewed at an accelerating voltage of 30 kV.

The atomic force microscopy in this study was manufactured by Shanghai AJ Nano-Science Development Limited (Shanghai, China) and operated in the tapping mode. RAP was diluted to the final concentration of 5 μg/mL in distilled water. 5 μL of solutions was dropped onto freshly cleaved mica and allowed to stand in air before imaging. The quoted spring constant was between 5.5 and 25 N m^{-1}.

2.10. Immunomodulatory activities of RAP on human peripheral blood mononuclear cells (PBMC)

Immunomodulatory activities of RAP were determined by the capacity of the compounds to influence the cytokine production by human PBMC. PBMCs were obtained from the buffy coat collected from Hong Kong Red Cross by density gradient separation. Buffy coat was diluted 1:1 with phosphate buffer saline (PBS) and this was overlaid on Ficoll Paque Plus (Amersham Biosciences). Cells were washed with PRMI and plated in 96-well plates at 10^5 cells/well. Serial dilutions of RAP from 10 to 10,000 ng/mL were added to the wells. The plates were maintained in a 37 °C incubator for 24 h. The immunomodulatory effects on PBMC of RAP were compared with a well known mitogen lipopolysaccharide (LPS) from Gram negative bacteria. The cell free supernatants were then assayed for GM-CSF (granulocyte-macrophage colony-stimulating factor), IFN (interferon)-γ, IL (interleukin)-1β, IL-2, IL-4, IL-10 IL-12 and TNF (tumor necrosis factor)-α production by commercially available human cytokine ELISA kits (BD OptEIA, USA) according to the manufacturer instruction with detection limits ranged from 3.1 to 7.8 pg/mL.

3. Results and discussion

3.1. Isolation and purification of RAP

RAP was purified from the crude polysaccharide RACP through a Hiload 26/60 Superdex-200 column. It presented a single and symmetrical peak in GPC (gel-permeation chromatography) examination on an Ultrahydrogel™ 1000 column (Fig. 1). The average molecular weight was 1334 kDa with reference to Dextran T-series standard samples of known molecular weight. The total sugar content was determined to be 76.5% using the phenol-sulfuric acid method. It had a high specific rotation of $[\alpha]_D^{20}$ +125.8 (0.54, H_2O) and weak UV absorption at 280 nm which was consistent with its low protein content (only 0.72%). The uronic acid content was 56.7% using colorimetric method.

3.2. Monosaccharide compositions analysis

After complete hydrolysis of RAP by 2 M TFA, its monosaccharide composition was determined using GC–MS. As demonstrated in Table 1, RAP contained Rha, Ara, Glc and Gal. Reduction of RAP with CMC-$NaBH_4$ gave the carboxyl-reduced derivative RAP-R and further analysis of RAP and RAP-R both indicated the presence of GalA. The molar ratio of Rha, Ara, Glc, Gal and GalA of RAP was 0.03:1.00:0.27:0.36:0.30, in which the ration of GalA was calculated by the increase of Gal content in RAP-R.

Table 1
Monosaccharide composition of RAP, RAP-R (RAP after reduction), RAP-P-H, RAP-P-L, and RAP-P-L-NH. RAP, after partially hydrolysis followed by dialysis, gave two parts: RAP-P-H (the part in the dialysis bag) and RAP-P-L (the part outside of the dialysis bag). RAP-P-L-NH meant direct examination on the monosaccharides in RAP-P-L before complete hydrolysis. The results were obtained on a Shimadzu GC/MS-QP2010 series coupled with a DB-5 ms capillary column (0.25 μm × 0.25 μm × 30 m).

Samples	Mw (kDa)	Monosaccharide composition (molar, %)			
		Rha	Ara	Glc	Gal
RAP	1334	0.03 (1.8)	1.00 (60.2)	0.27 (16.3)	0.36 (21.7)
RAP-R	n.d.	0.01 (0.6)	1.00 (55.6)	0.13 (7.2)	0.66 (36.7)
RAP-P-H	1215	0.28 (5.4)	1.00 (19.2)	1.84 (35.3)	2.00 (38.4)
RAP-P-L	n.d.	n.d.	1.00 (89.3)	0.10 (8.9)	0.02 (1.8)
RAP-P-L-NH	n.d.	n.d.	1.00 (100.0)	n.d.	n.d.

n.d. not determined.

3.3. Methylation analysis

RAP and RAP-R were methylated and analyzed by GC–MS in order to elucidate the linkages (Table 2). Compared with GalA's content given in monosaccharide composition analysis, the carboxyl-reduced RAP-R showed a significant increase of 1,4-linked Gal*p*, suggesting the GalA in RAP was 1,4-linked. Similarly, it could be suggested that RAP was mainly composed of T-linked Ara*f*, 1,5-linked Ara*f*, 1,4-linked Glc*p*, 1,4-linked GalA*p*, 1,3-linked Glc*p* and 1,3,6-linked Gal*p*. The terminals consisted of Ara*f* (20.6%), Glc*p* (2.0%) and Gal*p* (5.2%), indicating RAP was significantly branched and the side chains were terminated by the Ara residues.

The ratio of T-, 1,5- and 1,3,5-linked Ara*f* (50.9:41.7:7.4) suggested that the Ara side chains contained a central core of 1,5-linked Ara*f* residues. The high proportion of T-linked Ara*f* residues suggested that some terminal Ara residues existed in the Ara side chains, and others were attached to the highly branched Gal side chains or connected to the back bone directly (Ros, Schols, & Voragen, 1996; Sun, Cui, Tang, & Gu, 2010).

The proportion of terminal, 1,4-, 1,3-, 1,6-, 1,2,4-, 1,4,6- and 1,3,6-linked Gal*p* was 9.3:8.7:16.1:8.1:5.0:11.1:41.6. The low proportion of terminal residues of Gal (9.3%) indicated that a part of the Gal side chains were terminated by the Ara residues. The Rha residues were exclusively 1,2,4-linked. Glc residues were mainly terminal, 1,4-linked units, with a small amount of 1,3,4-linked

Table 2
GC–MS analysis for methylation of RAP, RAP-R and RAP-P-H on a DB-5 ms capillary column (0.25 μm × 0.25 μm × 30 m).

PMAA[a]	Molar ratios[b]			Linkages[c]
	RAP	RAP-R	RAP-P-H	
2,3,5-Me_3-Ara	13.4	20.6	4.2	T-
2,3-Me_2-Ara	10.9	19.8	9.0	1,5-
2-Me-Ara	2.0	4.3	–	1,3,5-
3-Me-Rha	3.9	5.8	3.9	1,2,4-
2,3,4,6-Me_4-Glc	4.4	2.0	4.2	T-
2,3,6-Me_3-Glc	24.3	15.3	30.1	1,4-
2,6-Me_2-Glc	1.9	1.7	3.9	1,3,4-
2,3,4,6-Me_4-Gal	3.6	5.2	7.5	T-
2,3,6-Me_3-Gal	3.4	14.4	3.3	1,4-
2,4,6-Me_3-Gal	6.3	2.0	14.2	1,3-
2,3,4-Me_3-Gal	3.2	1.8	6.9	1,6-
3,6-Me_2-Gal	1.9	0.8	–	1,2,4-
2,3-Me_2-Gal	4.4	2.1	5.1	1,4,6-
2,4-Me_2-Gal	16.3	4.1	7.5	1,3,6-

–, not determined.

[a] The sugar type was confirmed both with the literature and mass spectrum analysis.

[b] Molar ratios were given as percentage of total ion count (TIC).

[c] The pyranosyl or furanosyl forms of glycosyl residues was confirmed with ^{13}C NMR.

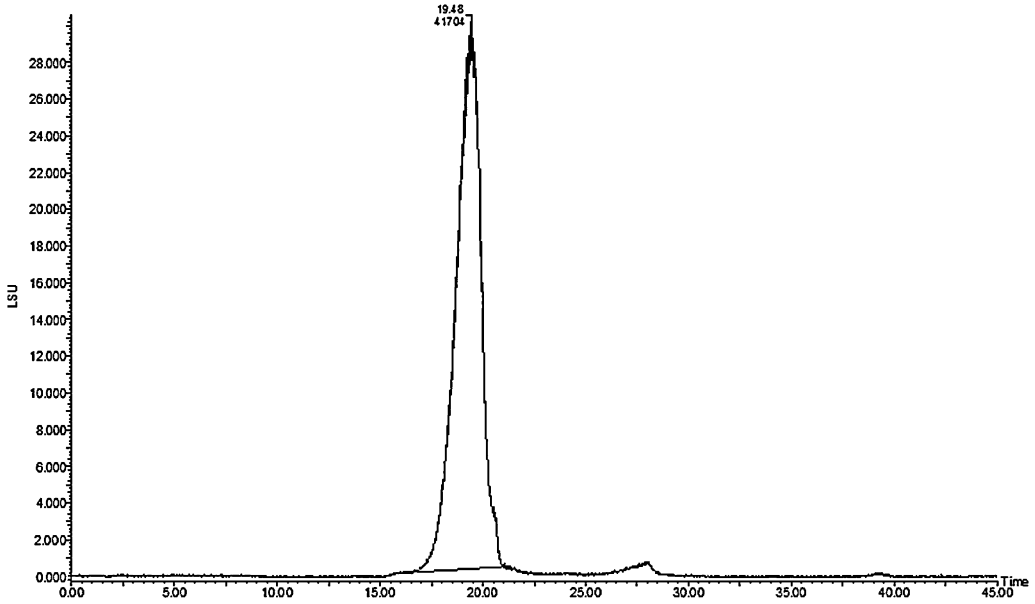

Fig. 1. GPC chromatogram of RAP on an Ultrahydrogel™ 1000 column (7.8 mm × 300 mm), mobile phase: water, at a flow rate of 0.3 mL/min, the ELS Detector conditions were: drift tube temperature (75 °C), nebulizer temperature (48 °C), gain (300 °C), gas pressure (45 Psi).

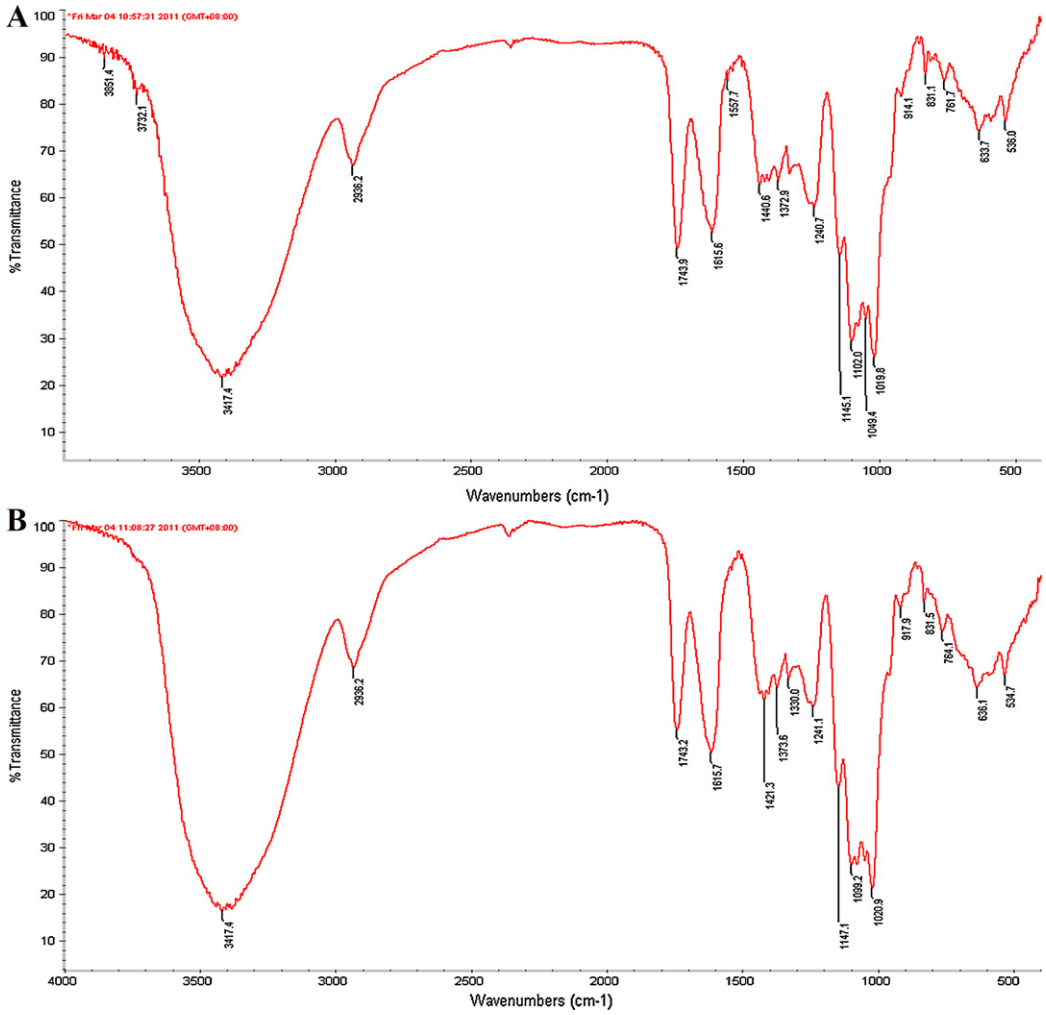

Fig. 2. The IR spectra of RAP (A) and RAP-P-H (B, partially hydrolyzed RAP), recorded in KBr tablet at the absorbance mode from 4000 to 400 cm^{-1} (mid infrared region) at a resolution of 4 cm^{-1}.

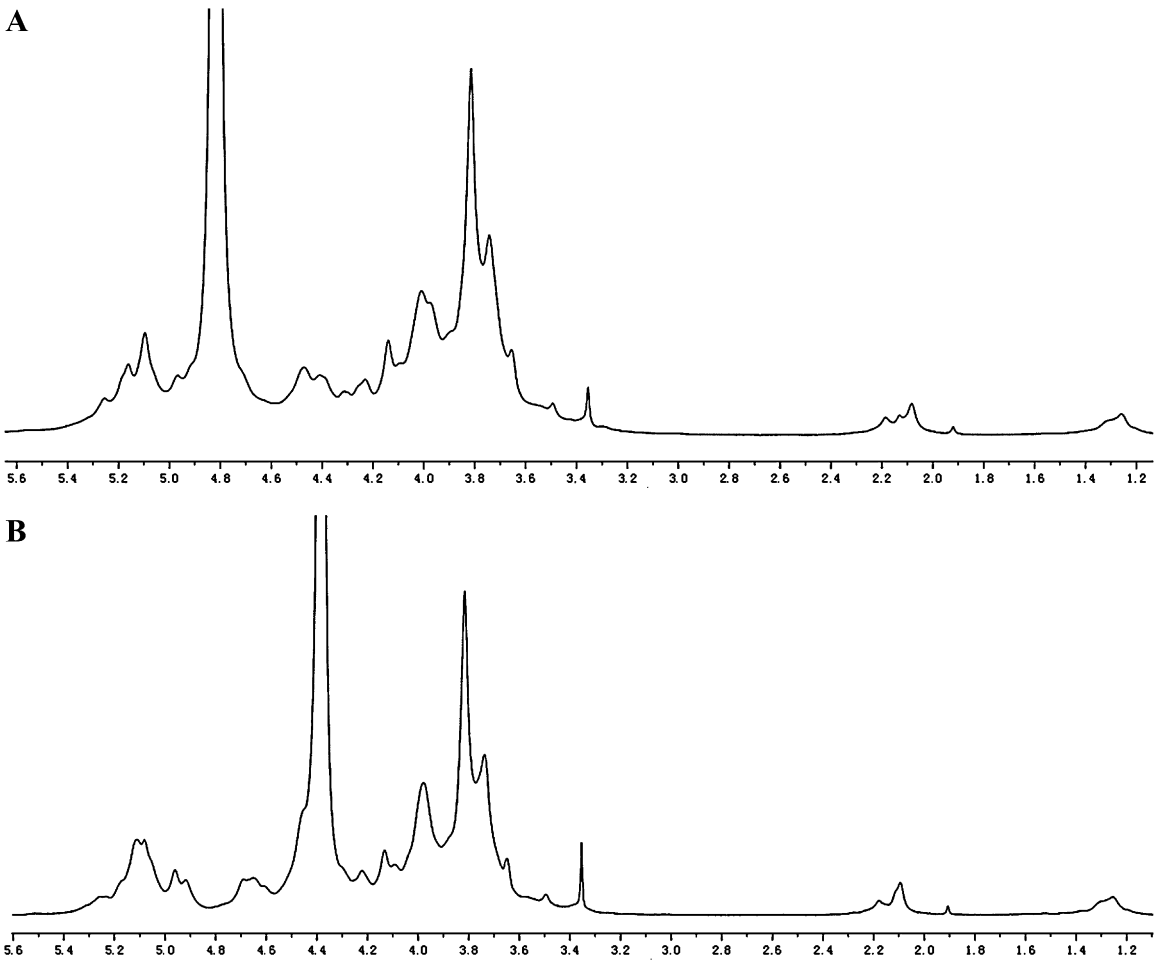

Fig. 3. The ^{1}H NMR (600.1 MHz) spectrum of RAP that was measured in a 5-mm NMR tube with 0.5 mL of 99.9% D_2O. (A) At 27 °C; (B) at 50 °C.

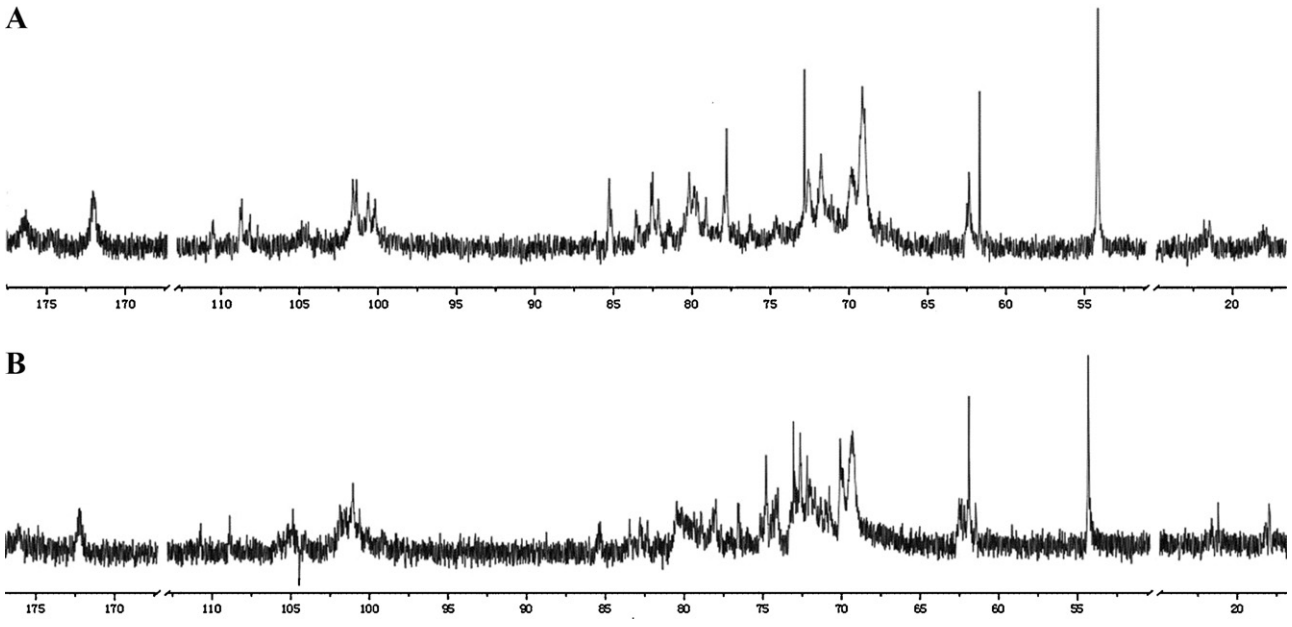

Fig. 4. The ^{13}C NMR (151.0 MHz) spectra of RAP (A) and RAP-P-H (B, partially hydrolyzed RAP) that were measured in a 5-mm NMR tube with 0.5 mL of 99.9% D_2O.

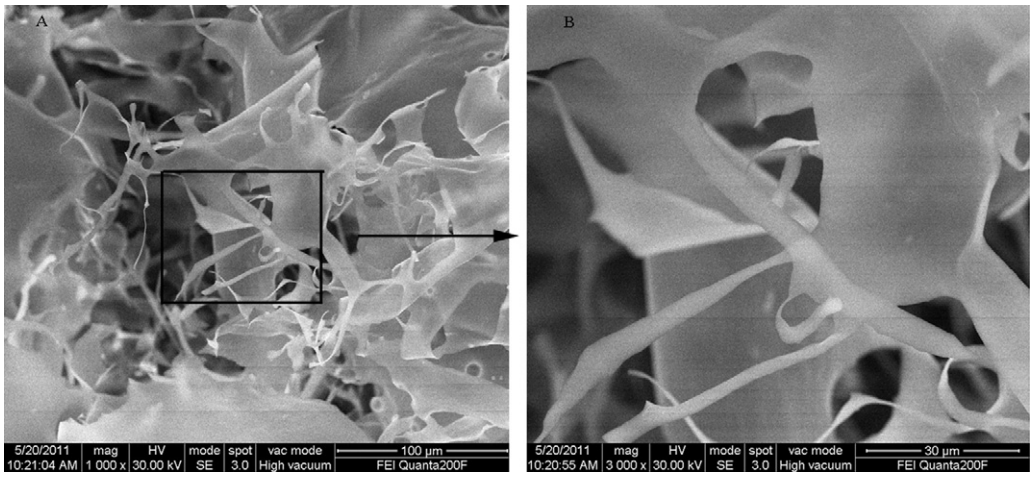

Fig. 5. SEM images of RAP at 1000× (A) and 3000× (B). The molecular morphology of RAP was first coated with a thin layer of gold, then observed using SEM at an accelerating voltage of 30 kV.

units. RAP contained two types of intra-chain linkages for galactose, a 1,4-linked that is common in type I arabinogalactan, and a 1,3,6-linked in type II arabinogalactan, suggesting that RAP contain different types of Gal branches.

3.4. Partial acid analysis

Partial degradation of polysaccharide by acid hydrolysis is based on the fact that some glycosidic linkages are tolerable to acid. To determine more structural features, RAP (50.5 mg) was partially hydrolyzed with 0.1 M TFA to give two parts, RAP-P-H (in the dialysis bag) and RAP-P-L (outside of the dialysis bag). Direct examination on the monosaccharides in RAP-P-L found only Ara, while after complete hydrolysis it gave a small amount of Glc (9.0%) and Gal (2.1%) in addition to Ara (88.8%) (Table 1). It was suggested that RAP probably contained terminal residues of Ara in the branch areas. There was no GalA found in RAP-P-L in HPLC examination (Honda et al., 1989), which confirmed that GalA was located in the backbone of RAP. These results suggested that GalA and Rha existed in the backbone and the neutral sugars were located in the side chains.

ESI-MS of RAP-P-L presented sodium cationized pseudomolecular ions at *m/z* 1159.9 $[Ara_6(Glc/Gal)_2+Na]^+$, 997.3 $[Ara_6(Glc/Gal)+Na]^+$, 702.0 $[Ara_5+Na]^+$, 569.1 $[Ara_4+Na]^+$, 407.1 $[Ara_3+Na]^+$ and 305.1 $[Ara_2+Na]^+$. RAP-P-L seemed a mixture of monosaccharide (terminal Ara residues) and oligosaccharide (containing [Ara-Ara] linkages).

The degraded polysaccharide RAP-P-H (30 mg) was mainly composed of Gal and Glc, with small amounts of Rha and Ara (Table 1). Its average molecular weight was 1215 kDa. The methylation analysis (Table 2) showed that the removal of most Ara*f* residues resulted in an increase of the ratio of 1,6-linked Gal*p* and significant increase for 1,3-linked Gal*p*. Therefore it could be deduced that Ara residues were attached to 1,6-linked and mainly 1,3-linked Gal residues. RAP-P-H gave no 1,3,5-linked Ara*f*, suggesting that 1,3,5-linked Ara*f* should be in the branch. A great amount of 1,4-linked Glc*p* residues still detected in RAP-P-H indicated that 1,4-linked Glc*p* residues were located in the backbone of RAP.

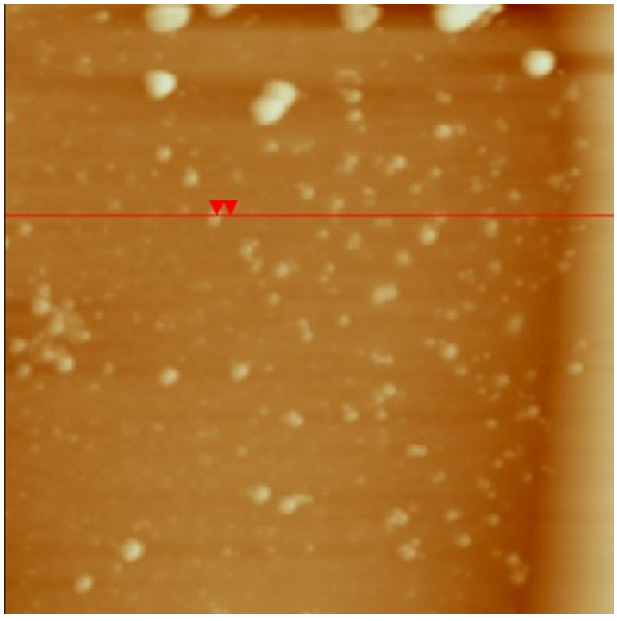

Fig. 6. AFM image of RAP. RAP was dissolved in distilled water at the concentration of 5 μg/mL. 5 μL of solution was dropped onto freshly cleaved mica and allowed to stand in air before imaging.

3.5. FT-IR spectra analysis

The IR spectrum of RAP (Fig. 2A) showed a strong band at 3404 cm^{-1} which was attributed to the hydroxyl stretching vibration of the polysaccharide. The band at 2935 cm^{-1} was due to C–H stretching vibration. Bands at 1743 and 1618 cm^{-1} indicated the ester carbonyl (COOR) groups and carboxylated ion groups (COO^-) (Gnanasambandam & Proctor, 2000). The FT-IR spectrum of RAP showed a strong absorbance at 1021, 1100 and 1142 cm^{-1} attributed to the stretching vibrations of α-pyranose ring of the glucosyl residue. Moreover, the characteristic absorptions at 830 and 916 cm^{-1} indicated that both α- and β-configurations existed. These observations confirmed that the RAP was a polysaccharide containing uronic acid.

The IR spectrum of RAP-P-H (Fig. 2B) showed the same characteristic absorption with RAP which indicated RAP-P-H retained the backbone of RAP.

3.6. NMR analysis

Signals in the ^1H and ^{13}C NMR spectra of RAP were assigned as much as possible, according to monosaccharide compositions analysis, methylation results and literature values (Bock, Pedersen, & Pedersen, 1984; Chandra, Ghosh, Ojha, & Islam, 2009; Polle,

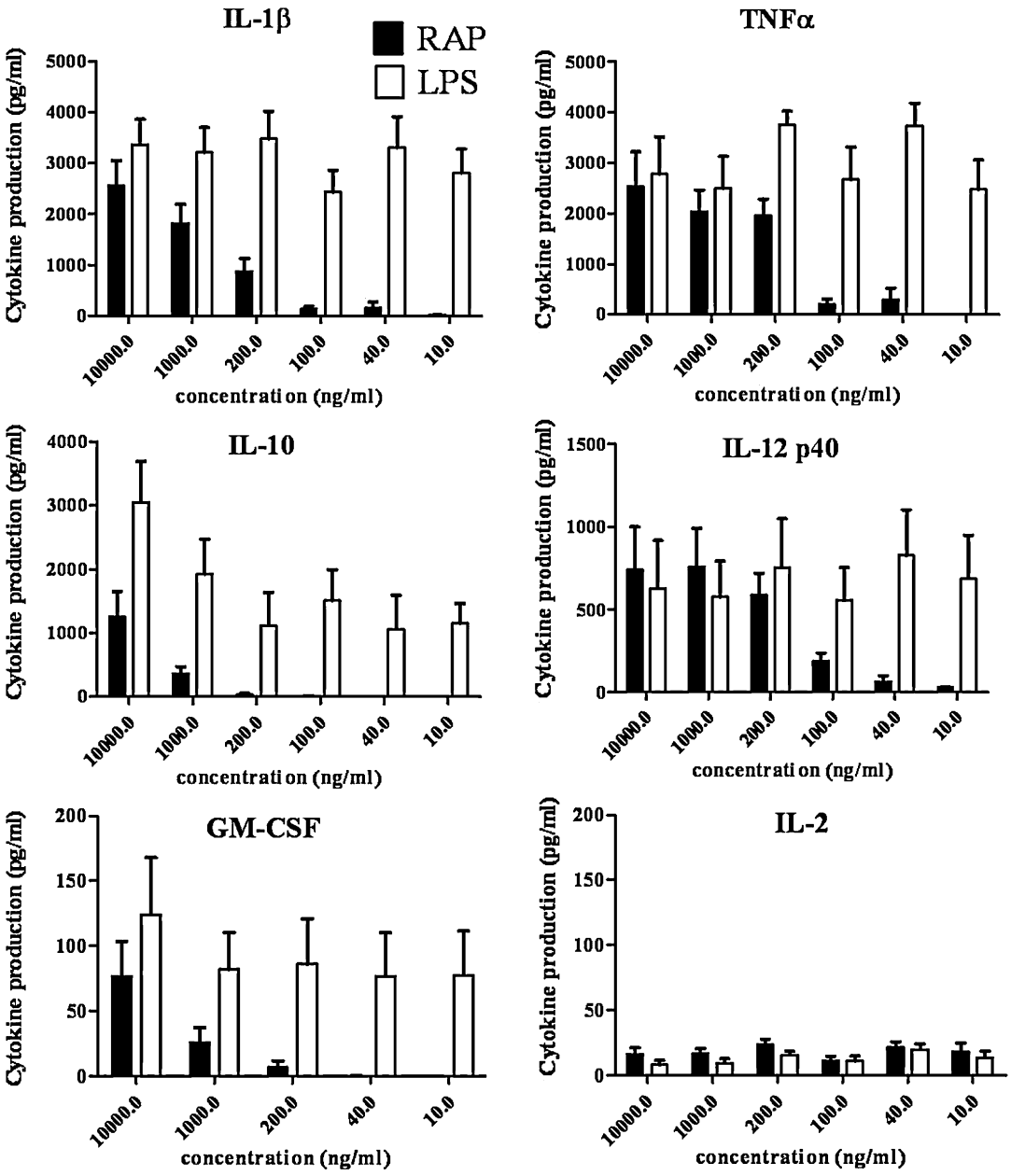

Fig. 7. Cytokines production (GM-CSF, IFN-γ, IL-1β, IL-2, IL-4, IL-10 IL-12 and TNF-α) of human blood mononuclear cells (PBMC) with the addition of RAP or LPS from 2 to 10,000 ng/mL. Each bar represents the mean ± SEM of duplicates ($n = 7$).

Ovodova, Shashkov, & Ovodov, 2002; Sun et al., 2010; Xu, Dong, Qiu, Cong, & Ding, 2010). The ^{1}H NMR spectrum (Fig. 3A) showed signals in the anomeric region. Due to the existence of H_2O in the sample or HDO from D_2O, there was large signal at δ 4.815 ppm which disturbed the analysis of RAP. Therefore, another ^{1}H NMR spectrum was obtained at 50 °C (Fig. 3B).

From methylation analysis, 1,4-linked Glc*p* was the main resides in RAP. So the signal at δ 5.096 ppm was assigned to α-1,4-linked Glc*p*. The signal at δ 5.254 ppm was assigned to α-1,5-linked Ara*f*, and the signal at δ 5.162 ppm was originated from α-1,3,5-linked Ara*f*. The signal at δ 4.968 ppm was assigned to α-1,4-linked GalA*p*6Me, which meant some of 1,4-linked GalA*p* was present as methyl ester. The signal at δ 4.922 could be assigned to α-1,4-linked GalA*p*. The signals at δ 4.693 and 4.653 ppm were assigned to β-1,3,6-linked Gal*p*. The signal at δ 4.469 ppm was assigned to β-1,3-linked Gal*p* and corresponded with β-1,3-linked Gal*p* anomeric carbon resonance at δ 104.43 ppm in the HSQC. The proton signals nearby δ 2.083, 2.131 and 2.186 ppm could be assigned from the $-CH_3$ of the *O*-acetyl groups. It suggested that RAP contained kinds of *O*-acetyl groups at the different positions of the sugar residues or different chemical environments. Signal at δ 1.260 ppm was identified to be H-6 from methyl group of the Rha residues. The overlapped signals in the range of δ 3.355–4.410 ppm were assigned to protons H-2 to H-5 (or H-6) of the glycosidic ring.

The anomeric signals in the ^{13}C NMR spectrum of RAP (Fig. 4A) were assigned partly according to correlations in the HSQC spectrum. The signal at δ 108.66 ppm correlated to H-1 (δ 108.66/5.096 ppm) of T-Ara*f*. The signal at δ 110.48 ppm coupled to H-1 (δ 110.48/5.254 ppm) of 1,5-linked Ara*f*. The signal at δ 108.13 ppm corresponded to 1,3,5-linked Ara*f*, which was confirmed by its absence in the ^{13}C NMR spectrum of RAP-P-H (Fig. 4B). The low-field chemical shifts indicated the Ara residues were in furanose form and adopted α-anomeric configuration (Xu et al., 2010). Methylation analysis results showed that 1,3-linked

Gal*p* residues increased significantly after partial acid hydrolysis of RAP. Compared with the ^{13}C NMR of RAP, signal at δ 104.43 ppm became much stronger in RAP-P-H. So the signal at δ 104.43 ppm (δ 104.43/4.469 ppm from HSQC) was assigned to 1,3-linked Gal*p*. The signal at δ 101.37 ppm was assigned to C-1 of 1,4-linked GalA*p*. The signals at δ 101.60 and 100.18 ppm were assigned to C-1 of 1,3,6-linked Gal*p* and α-1,4-linked GalA*p*6Me. And the signal at δ 100.61 ppm was assigned to C-1 of 1,4-linked Glc*p*. The signal at δ 62.36 ppm was assigned to C-5 of a terminal Ara, while the stronger signal at δ 61.68 ppm was attributed to the C-6 of 1,4-linked Glc*p*.

The signal at δ 18.06 ppm could be assigned to the methyl carbon of Rha. The signal at δ 54.15 ppm could be assigned to methyl ester groups of RAP. The presence of methyl esterified GalA*p* was also supported by the signals at δ 54.15/3.814 ppm in HSQC spectrum (Bushneva, Ovodova, Shashkov, & Ovodov, 2002). In the low field, typical signals for the C-6 carboxyl group of GalA were observed at δ 176.33 and 172.06 ppm, which confirmed the presence of free and esterified carboxyl groups of GalA. RAP and RAP-R after hydrolysis were acetylated, and no methylated monosaccharide was detected by GC–MS (Samuelsen et al., 1999). It was confirmed that the 1,4-linked GalAp was present as 1,4-linked GalAp6Me.

3.7. Molecular morphology of RAP

Its molecular morphology was further investigated by scanning electron microscopy (SEM) and atomic force microscopy (AFM). The SEM micrograph of RAP was shown in Fig. 5. RAP appeared as loose flaky and curly aggregation. The observed irregular microstructure demonstrated that RAP was a type of amorphous solid.

The molecular morphology of RAP was further investigated by single molecular AFM. The topographical image was shown in Fig. 6. The results showed that there were many spherical lumps within the height of 3–70 nm while the height of a single polysaccharide chain is generally 0.1–1 nm, which suggested molecular aggregation happened somehow. There might be a repulsive force between the polysaccharide and the mica causing aggregation (Chen et al., 2009) because both RAP and the mica a type of aluminum silicate were negative. The side chains might be another reason for the aggregation (Sletmoen, Maurstad, Sikorski, Paulsen, & Stokke, 2003).

3.8. Immunomodulatory activities on human peripheral blood mononuclear cells (PBMC)

RAP has been investigated for its *in vitro* effect on the cytokine profile (GM-CSF, IFN-γ, IL-1β, IL-2, IL-4, IL-10, IL-12 and TNF-α) of unstimulated human PBMC compared with LPS. No significant productions of cytokines were detected in drug free negative control. When RAP was added to RPMI for 24 h incubations, potent stimulatory effects on the production of two pro-inflammatory cytokines IL-1β and TNF-α from PBMC were observed from 200 to 10,000 ng/mL (Fig. 7). These cytokines are important in mediating the immune response against bacterial infections. Dose dependent stimulation of IL-10, IL-12 and GM-CSF productions from PBMC were also observed with RAP addition but the stimulatory activities was not weaker than LPS. The source of these 5 cytokines is mainly from monocytes and these results suggested that RAP is an activator of monocytes and further studies are required to investigate its mechanism of action such as the involvement of toll like receptors. For T cell producing cytokines (IL-2, IL-4 and IFN-γ), RAP did not produce any significant effects on PBMC (Fig. 7).

4. Conclusion

A water soluble polysaccharide (RAP), with the average molecular weight 1334 kDa, was isolated from Radix Astragali. It was composed of Rha, Ara, Glc, Gal and GalA in a molar ratio of 0.03:1.00:0.27:0.36:0.30. The structure was characterized by partial acid hydrolysis, methylation analysis, FT-IR, GC–MS and ^{1}H and ^{13}C NMR analysis. The backbone of RAP mainly consisted of 1,2,4-linked Rha*p*, α-1,4-linked Glc*p*, α-1,4-linked GalA*p*6Me, β-1,3,6-linked Gal*p*. It had branches at *O*-4 of the 1,2,4-linked Rha*p* and *O*-3 or *O*-6 of β-1,3,6-linked Gal*p*. The side chains mainly consisted of α-T-Ara*f* and α-1,5-linked Ara*f* possessing *O*-3 as branching points, with trace Glc and Gal. The terminal residues were T-linked Ara*f*, T-linked Glc*p* and T-linked Gal*p*. Morphology analysis using SEM and AFM showed that RAP took random coil feature. This hyperbranched heteroglycan exhibited significant immunomodulating effects by stimulating the cytokines production mainly from monocytes in a dose dependent manner.

Acknowledgement

This research is funded by the Innovation and Technology Fund (ITS/311/09 and InP/108/10) of the Government of the Hong Kong Special Administrative Region.

References

Bedir, E., Pugh, N., Calis, I., Pasco, D. S., & Khan, I. A. (2000). Immunostimulatory effects of cycloartane-type triterpene glycosides from Astragalus species. *Biological & Pharmaceutical Bulletin*, *23*(7), 834–837.

Blumenkr, N., & Asboehan, G. (1973). New method for quantitative determination of uronic acids. *Analytical Biochemistry*, *54*(2), 484–489.

Bock, K., Pedersen, C., & Pedersen, H. (1984). Carbon-13 nuclear magnetic resonance data for oligosaccharides. *Advances in Carbohydrate Chemistry and Biochemistry*, *42*, 193–225.

Bradford, M. M. (1976). A rapid and sensitive method for the quantitation of protein utilizing the principle of protein-dye binding. *Analytical Biochemistry*, *72*(1–2), 248–254.

Bushneva, O. A., Ovodova, R. G., Shashkov, A. S., & Ovodov, Y. S. (2002). Structural studies on hairy region of pectic polysaccharide from campion *Silene vulgaris* (Oberna behen). *Carbohydrate Polymers*, *49*(4), 471–478.

Chan, J. Y. W., Lam, F. C., Leung, P. C., Che, C. T., & Fung, K. P. (2009). Antihyperglycemic and antioxidative effects of a herbal formulation of Radix Astragali Radix Codonopsis and Cortex Lycii in a mouse model of type 2 diabetes mellitus. *Phytotherapy Research*, *23*(5), 658–665.

Chandra, K., Ghosh, K., Ojha, A. K., & Islam, S. S. (2009). Chemical analysis of a polysaccharide of unripe (green) tomato (*Lycopersicon esculentum*). *Carbohydrate Research*, *344*(16), 2188–2194.

Chen, Y., Xie, M. Y., Nie, S. P., Li, C., & Wang, Y. X. (2008). Purification, composition analysis and antioxidant activity of a polysaccharide from the fruiting bodies of *Ganoderma atrum*. *Food Chemistry*, *107*(1), 231–241.

Chen, H. X., Wang, Z. S., Qu, Z. S., Fu, L. L., Dong, P., & Zhang, X. (2009). Physicochemical characterization and antioxidant activity of a polysaccharide isolated from oolong tea. *European Food Research and Technology*, *229*(4), 629–635.

Choi, S. I., Heo, T. R., Min, B. H., Cui, J. H., Choi, B. H., & Park, S. R. (2007). Alleviation of osteoarthritis by calycosin-7-O-beta-D-glucopyranoside (CG) isolated from Astragali Radix (AR) in rabbit osteoarthritis (OA) model. *Osteoarthritis and Cartilage*, *15*(9), 1086–1092.

Chu, C., Qi, L. W., Li, B., Gao, W., & Li, P. (2010). Radix Astragali (Astragalus): Latest advancements and trends in chemistry, analysis, pharmacology and pharmacokinetics. *Current Organic Chemistry*, *14*(16), 1792–1807.

Ciucanu, I., & Kerek, F. (1984). A simple and rapid method for the permethylation of carbohydrates. *Carbohydrate Research*, *131*(2), 209–217.

Dubois, M., Gilles, K. A., Hamilton, J. K., Rebers, P. A., & Smith, F. (1956). Colorimetric method for determination of sugars and related substances. *Analytical Chemistry*, *28*(3), 350–356.

Fang, J. N., & Wagner, H. (1988). Chemical structure of a glucan from *Astragalus mongholicus*. *Acta Chimica Sinica*, *46*(11), 1101–1104.

Gnanasambandam, R., & Proctor, A. (2000). Determination of pectin degree of esterification by diffuse reflectance Fourier transform infrared spectroscopy. *Food Chemistry*, *68*(3), 327–332.

Guo, Q., Cui, S. W., Wang, Q., & Christopher Young, J. (2008). Fractionation and physicochemical characterization of psyllium gum. *Carbohydrate Polymers*, *73*(1), 35–43.

Honda, S., Akao, E., Suzuki, S., Okuda, M., Kakehi, K., & Nakamura, J. (1989). High-performance liquid chromatography of reducing carbohydrates as strongly ultraviolet-absorbing and electrochemically sensitive 1-phenyl-3-methyl5-pyrazolone derivatives. *Analytical Biochemistry*, *180*(2), 351–357.

Jones, T. M., & Albersheim, P. (1972). A gas chromatographic method for the determination of aldose and uronic acid constituents of plant cell wall polysaccharides. *Plant Physiology*, *49*(6), 926.

Kiyohara, H., Uchida, T., Takakiwa, M., Matsuzaki, T., Hada, N., Takeda, T., et al. (2010). Different contributions of side-chains in beta-D-(1 → 3,6)-galactans on intestinal Peyer's patch-immunomodulation by polysaccharides from *Astragalus mongholics* Bunge. *Phytochemistry*, *71*(2–3), 280–293.

Lee, K. Y., & Jeon, Y. J. (2005). Macrophage activation by polysaccharide isolated from *Astragalus membranaceus*. *International Immunopharmacology*, *5*(7–8), 1225–1233.

Li, S. G., & Zhang, Y. Q. (2009). Characterization and renal protective effect of a polysaccharide from *Astragalus membranaceus*. *Carbohydrate Polymers*, *78*(2), 343–348.

Polle, A. Y., Ovodova, R. G., Shashkov, A. S., & Ovodov, Y. S. (2002). Some structural features of pectic polysaccharide from tansy *Tanacetum vulgare* L. *Carbohydrate Polymers*, *49*(3), 337–344.

Ros, J. M., Schols, H. A., & Voragen, A. G. J. (1996). Extraction, characterisation, and enzymatic degradation of lemon peel pectins. *Carbohydrate Research*, *282*(2), 271–284.

Samuelsen, A. B., Lund, I., Djahromi, J. M., Paulsen, B. S., Wold, J. K., & Knutsen, S. H. (1999). Structural features and anti-complementary activity of some heteroxylan polysaccharide fractions from the seeds of Plantago major L. *Carbohydrate Polymers*, *38*(2), 133–143.

Shao, B. M., Xu, W., Dai, H., Tu, P. F., Li, Z. J., & Gao, X. M. (2004). A study on the immune receptors for polysaccharides from the roots of *Astragalus membranaceus*, a Chinese medicinal herb. *Biochemical and Biophysical Research Communications*, *320*(4), 1103–1111.

Shimizu, N., Tomoda, M., Kanari, M., & Gonda, R. (1991). An acidic polysaccharide having activity on the reticuloendothelial system from the root of *Astragalus mongholicus*. *Chemical & Pharmaceutical Bulletin*, *39*(11), 2969–2972.

Sletmoen, M., Maurstad, G., Sikorski, P., Paulsen, B. S., & Stokke, B. T. (2003). Characterisation of bacterial polysaccharides: Steps towards single-molecular studies. *Carbohydrate Research*, *338*(23), 2459–2475.

Staub, A. M. (1965). Removal of protein-Sevag method. *Methods in Carbohydrate Chemistry*, *5*, 5–6.

Sun, Y., Cui, S. W., Tang, J., & Gu, X. (2010). Structural features of pectic polysaccharide from *Angelica sinensis* (Oliv.) Diels. *Carbohydrate Polymers*, *80*(2), 544–550.

Taylor, R. L., & Conrad, H. E. (1972). Stoichiometric depolymerization of polyuronides and glycosaminoglycuronans to monosaccharides following reduction of their carbodiimide-activated carboxyl group. *Biochemistry*, *11*(8), 1383–1388.

Wang, S. C., Shan, J. J., Wang, Z. T., & Hu, Z. B. (2006). Isolation and structural analysis of an acidic polysaccharide from *Astragalus membranaceus* (Fisch.) Bunge. *Journal of Integrative Plant Biology*, *48*(11), 1379–1384.

Wang, Z. F., He, Y., & Huang, L. J. (2007). An alternative method for the rapid synthesis of partially O-methylated alditol acetate standards for GC–MS analysis of carbohydrates. *Carbohydrate Research*, *342*(14), 2149–2151.

Xu, Y. X., Dong, Q., Qiu, H., Cong, R. H., & Ding, K. (2010). Structural characterization of an arabinogalactan from platycodon grandiflorum roots and antiangiogenic activity of its sulfated derivative. *Biomacromolecules*, *11*(10), 2558–2566.

Yan, H., Xie, Y. P., Sun, S. G., Sun, X. D., Ren, F. X., Shi, Q. R., et al. (2010). Chemical analysis of *Astragalus mongholicus* polysaccharides and antioxidant activity of the polysaccharides. *Carbohydrate Polymers*, *82*(3), 636–640.

Yin, F. G., Liu, Y. L., Yin, Y. L., Kong, X. F., Huang, R. L., Li, T. J., et al. (2009). Dietary supplementation with Astragalus polysaccharide enhances ileal digestibilities and serum concentrations of amino acids in early weaned piglets. *Amino Acids*, *37*(2), 263–270.

Yu, D. H., Bao, Y. M., Wei, C. L., & An, L. J. (2005). Studies of chemical constituents and their antioxidant activities from *Astragalus mongholicus* Bunge. *Biomedical and Environmental Sciences*, *18*(5), 297–301.

Zhang, X.-J., Chen, G.-Z., Ke, M., Han, H., Lu, Z.-W., Wang, T.-J., et al. (2011). Study on *Astragalus mongholicus* polysaccharides: Molecule structure and antioxidant activities evaluation. *Carbohydrate Polymers*, *85*(2), 312–317.

Zhu, H. Y., Zhang, Y. Y., Ye, G., Li, Z. X., Zhou, P., & Huang, C. G. (2009). In vivo and in vitro antiviral activities of calycosin-7-O-beta-D-glucopyranoside against Coxsackie virus B3. *Biological & Pharmaceutical Bulletin*, *32*(1), 68–73.